Medical Engineering and Physics 95 (2021) 90–96

Contents lists available at ScienceDirect

Medical Engineering and Physics

journal homepage: www.elsevier.com/locate/medengphy

Technical note

Foot-surface-structure analysis using a smartphone-based 3D foot scanner

Tomoko Yamashita [a,*], Kazuhiko Yamashita [b], Mitsuru Sato [c], Masashi Kawasumi [d], Shingo Ata [a]

[a] Graduate School of Engineering, Osaka City University, 3-3-138 Sugimoto, Sumiyoshi-ku, Osaka 558-8585, Japan
[b] Department of Clinical Engineering, Faculty of Human Care at Makuhari, Tohto University, 1-1 Hibino, Mihama-ku, Chiba-shi, Chiba 261-0021, Japan
[c] School of Nursing and Rehabilitation Sciences, Showa University, 1865 Tokaichibacho, Midori-ku, Yokohama-shi, Kanagawa 226-8555, Japan
[d] School of Science and Technology for Future Life, Tokyo Denki University, 5 Senju Asahi-cho, Adachi-ku, Tokyo 120-8551, Japan

ARTICLE INFO

Keywords:
Foot 3D scanner
Smartphone
Hallux valgus

ABSTRACT [1]

Background: A thorough understanding of the influence of the foot skeletal structure on hallux valgus (HV) is required for HV prevention. We developed a system using a 3D foot scanner on a smartphone to clarify the relationships between foot features and HV risk.
Methods: Two-dimensional video images were recorded on a smartphone, sent to a computer or cloud server, and used to construct a 3D foot-feature model, considering 10 foot features associated with HV. The participants (419 individuals, aged 40–89 years) stood with their toes 12 cm apart and heels 8 cm apart during video recording. The height and weight were measured for body-mass index calculation.
Results: Age-dependent foot-feature variations were observed slightly for males and distinctively for females. For females, the great toe–first metatarsal head–heel (GFH) angle associated with HV increased with age, i.e., the GFH angle increased with age, suggesting that HV increased with age. Multiple regression analysis revealed that the features determining the GFH angle are the second toe–heel–navicular angle, bone distance axis, and transverse arch length and height. The adjusted coefficients of determination were 0.54 and 0.52 for males and females, respectively.
Conclusion: This approach enables simple foot structure assessment for HV risk evaluation.

1. Introduction

Hallux valgus (HV) is a common foot deformity characterized by abnormal angulation, rotation, and lateral deviation of the great toe at the first metatarsophalangeal joint. HV occurs widely across all age groups. It is most common (35.7%) in older adults aged above 65 years, followed by adults aged 18–65 years [1]. Moreover, its occurrence is higher in females (30%) than in males (13%) [1].

It has been reported that assessing the skeletal features of the human foot offers an effective means of HV diagnosis [2]. Moreover, HV occurrence is influenced by several factors, including gender [1,3], age [1], body-mass index (BMI) [2], first metatarsal length [4,5], existing flat feet condition [4], osteoarthritis [5,6], and footwear preferences [7]. However, the influence of the foot structure on HV remains poorly understood [8]. Given the high prevalence of HV, an early understanding of the skeletal features of the feet could play an important role in its mitigation or even prevention. Quantitative analysis of the foot shape is important for not only the clinical assessment of existing foot deformities [9] but also the realization of several applications such as ergonomic footwear design, foot orthotics, and insoles.

Foot-feature assessments can be performed using two major methods: laser-based 3D foot-surface scanning and X-ray analysis. Although the former approach is expensive, it is often used in the fabrication of custom-made shoes that perfectly match the foot shape of the customer [10,11]. More specifically, it is utilized to measure the length and circumference of the foot; however, no prior study has considered the use of this method for analyzing foot features in the presence of foot deformities such as HV. By contrast, X-ray analysis is invasive and can only be performed at medical institutions. In addition, X-ray scans, in principle, produce two-dimensional (2D) images, causing measurements performed via X-ray scanning to be error-prone owing to inconsistencies that may exist between the scanning angles considered.

* Corresponding author.
E-mail address: d19tb552@eb.osaka-cu.ac.jp (T. Yamashita).

[1] 2D: two-dimensional; 3D: three-dimensional; ABD: axis of the bone distance; BMI: body-mass index; GFH: great toe–first metatarsal head–heel; GSR: great toe–second toe ratio; HV: hallux valgus; IH: instep height; IS: instep; MPH: metatarsophalangeal heel; NH: navicular height; SHN: second toe–heel–navicular; TAH: transverse arch height; TAL: transverse arch length

https://doi.org/10.1016/j.medengphy.2021.08.001
Received 11 February 2021; Received in revised form 4 August 2021; Accepted 4 August 2021
Available online 10 August 2021

Further, such analyses are dependent on the X-ray operator. Nix et al. reported that HV cannot be adequately defined via X-ray scanning, and there are no means to make appropriate adjustments to eliminate significant differences between groups [11].

Telfer and Woodburn recently developed a 3D scanning technique that can be used to obtain information regarding the surfaces, volumes, and cross-sections of human body parts. Their technique facilitates the rapid scanning of numerous individuals, and they obtained robust and efficient measurement results [12]. Mall et al. compared the foot dimensions obtained using optical techniques and caliper measurements, and reported that the former was more reliable and less time-consuming than the latter [13]. Zhao et al. proposed an approach to measure the foot girth at six points to customize footwear; the results obtained revealed differences of less than 5 mm compared to manual measurements [14]. However, most of these studies were undertaken from a shoe design and fit perspective and not for evaluating foot deformities for HV diagnosis.

Therefore, a simple 3D foot-scanner system was developed in this study, whose implementation requires only a smartphone and a remote computer. The objective of this study was to identify the foot features of male and female participants belonging to different age groups. Some of these features could be considered as indices for HV risk evaluation.

2. Methods

2.1. Development of smartphone-based 3D foot-surface morphology scanner

In this study, we developed a 3D foot-scanner system capable of analyzing the features of a human foot. A key characteristic of this system is that the only hardware required for its implementation is a smartphone, which is a widely used device. Therefore, the proposed system can be employed by anyone familiar with the use of cameras built into smartphones. The acquisition of video sequences of the feet for measurement using a smartphone is depicted in Fig. 1.

The proposed system analyzes the foot features of the subject by sending the 2D video sequences recorded using the smartphone camera to a remote computer or cloud server. Accordingly, the proposed system does not require the use of sophisticated high-specification hardware. The video sequences can be recorded manually, as long as the foot being analyzed remains within the camera frame. The system affords users a spatial resolution of 1.7 mm in a well-equipped laboratory with a corresponding high reproducibility of results [15].

Figs. 2(a)–(d) define the foot features assessed in this study. The instep height (IH) is the distance between the sole and talus head at the highest instep point, the navicular height (NH) is the distance between the sole and navicular bone, and the instep (IS) angle is the angle formed between the hallux tip, talus head, and heel (Fig. 2(a)). The second toe–heel–navicular (SHN) angle is the angle between the second-toe tip, navicular bone, and heel (Fig. 2(b)). The transverse arch length (TAL) is the distance between the interior and exterior of the first and fifth metatarsal heads, respectively, whereas the transverse arch height (TAH) is the maximum distance between the sole and line touching the upper forefoot surface, thereby describing the TAL (see Fig. 2(c)). The metatarsophalangeal heel (MPH) angle is the angle between the interior of the first metatarsal head, heel, and exterior of the fifth metatarsal head. Further, the great toe–first metatarsal head–heel (GFH) angle is the angle between the hallux tip, interior of the first metatarsal head, and heel. Lastly, the axis of the bone distance (ABD) is the centerline distance between the heel and tip of the second toe when the talus-head coordinate is projected onto the floor (Fig. 2(d)). In addition, the great toe–second toe ratio (GSR), i.e., the ratio of the distance between the second-toe tip and heel to that between the hallux tip and heel, was determined to investigate the influence of toe length. It is noteworthy that these distance-based features are influenced by the foot length; i.e., the values of the aforementioned parameters vary depending on the size of the foot being analyzed. Accordingly, the values of these parameters were normalized with respect to the distance between the heel and hallux (i.e., foot length) and multiplied by 100. Furthermore, to investigate the influence of personal physique, the height and weight of each participant were measured for BMI calculation.

Based on the above foot-feature definitions, IH as well as TAL and TAH could be considered indices for measuring the transverse and lateral arches, respectively. Likewise, the SHN and GFH angles could be considered pronated foot and HV indicators, respectively.

Finally, ABD indicates the point at which the skeleton appears misaligned. It is noteworthy that the HV angle—i.e., the angle between the longitudinal axes of the first metatarsal and proximal phalanx—is used to grade HV severity clinically as mild (15°–20°), moderate (21°–39°), or severe (≥40°) [16]. In this study, the GFH angle was considered to be a substitute for the HV angle, which can be measured via X-ray only. In view of this identification of the GFH angle as a key foot feature, an estimation method is proposed in this paper. Table 1 summarizes the 10 above-described features.

2.2. Participants

This study was conducted in Shiki City, Saitama, Japan, which has a

Fig. 1. Acquiring video sequences of the feet for measurement.

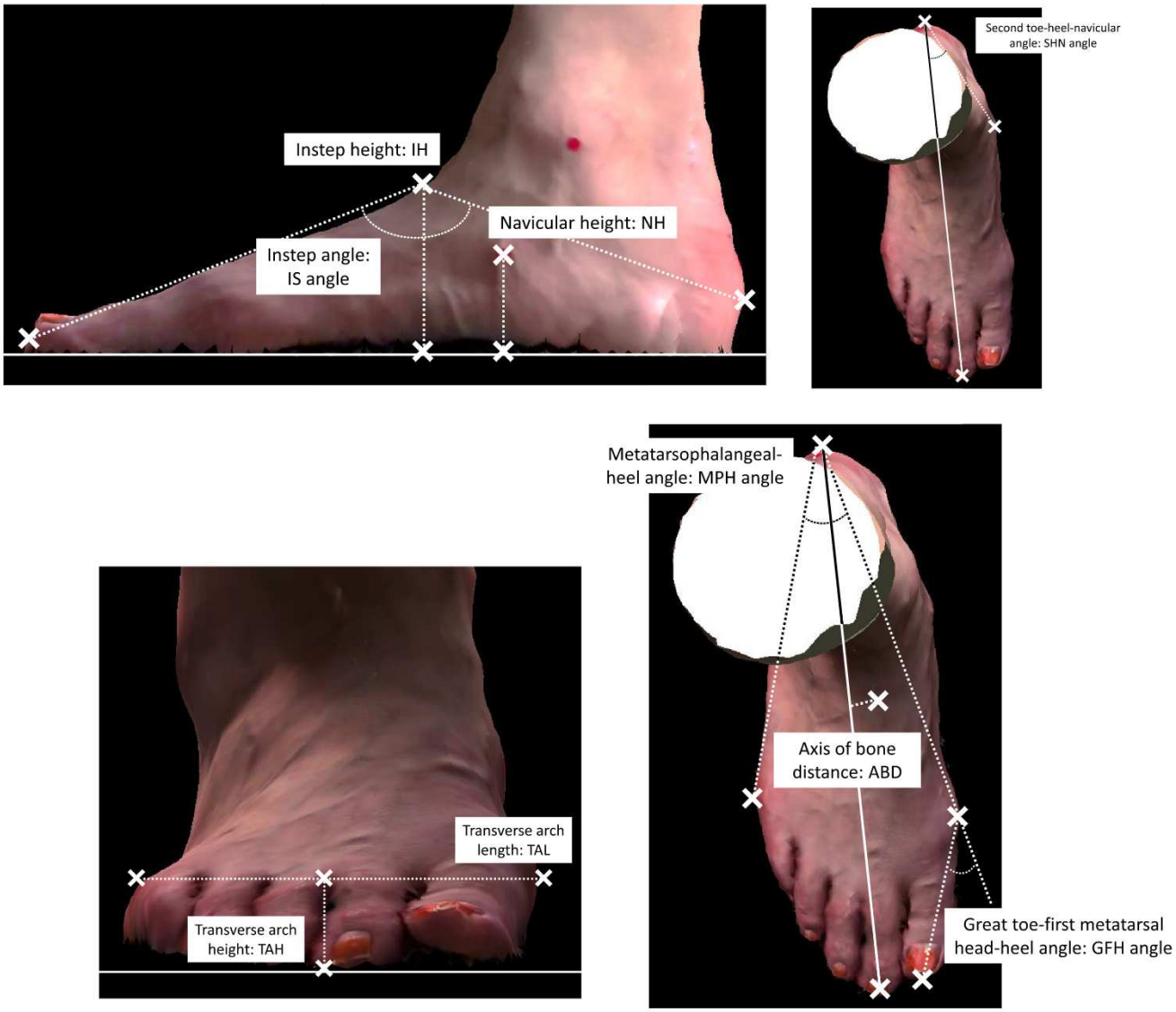

Fig. 2. (a, b, c, d).

population of approximately 76,000. In this study, participants were recruited via advertisements published by the public relations department of the city. Prior to the commencement of the foot-feature assessments, informed consent was obtained from all participants. The study design was approved by the ethical review board in the Ryotokuji University (Approval Number 1909).

The target participant group comprised 419 individuals (age: 40–89 years; mean age: 62.8 ± 12.4 years), including 151 males (mean age: 65.6 ± 11.0 years) and 268 females (mean age: 63.8 ± 12.4 years). Table 2 lists the details pertaining to the participants recruited in this study. The inclusion criteria were an age of 40–90 years and the ability to walk without assistance. The exclusion criteria included factors such as lower-limb musculoskeletal disorders, concomitant systemic diseases, clinical signs of joint laxity, and major lower-limb trauma.

2.3. Measurement methods

The measurements were performed using a commercially available smartphone—iPhone 6 (Apple Inc., USA). All participants were instructed to maintain a standing posture with their toes and heels positioned 12 and 8 cm apart, respectively, throughout the measurements. A volunteer in charge of performing the measurements scanned the feet of the participants by panning around them and recording approximately 12-s-long video sequences using the smartphone. Further, the foot-feature points of the participants identified by a physical therapist via palpation were noted by sticking on a 4-mm-diameter marker. It is noteworthy that, because the measurements performed on the left and right feet yielded identical results, the proposed 3D foot-surface model is exclusively based on the measurement results obtained for the right foot.

2.4. Statistical analysis

In this study, we used the SPSS software package (version 24; IBM SPSS Statistics) to analyze the measured data. During analysis, foot-feature comparisons were performed using the student's *t*-test for unpaired data. Moreover, statistically significant differences between measured foot features were assessed by performing a one-way Analysis of variance (ANOVA) and Tukey's post hoc test. The relationships between features were explored using Pearson's correlation coefficient. During the analysis, the GFH angle was considered equivalent to the HV angle, and multiple linear regression was used to identify the features strongly associated with the GFH angle, where a p value of 0.05 was considered statistically significant.

Table 1
Foot-feature definitions.

Abbreviation	Meaning	Definition
IH	Instep height	Distance between the sole and talus head at the highest instep point
NH	Navicular height	Distance between the sole and navicular bone
IS	Instep angle	Angle between the hallux tip, talus head, and heel
SHN angle	Second toe–heel–navicular angle	Angle between second-toe tip, navicular bone, and heel
TAL	Transverse arch length	Distance between the interior of the first metatarsal head and exterior of the fifth metatarsal
TAH	Transverse arch height	Maximal distance between the sole and line on the metatarsals yielding TAL
MPH angle	Metatarsophalangeal heel angle	Angle between the interior of the first metatarsal head, heel, and exterior of the fifth metatarsal head
GFH angle	Great toe–first metatarsal head–heel angle	Angle between the hallux tip, interior of first metatarsal head, and heel
ABD	Axis of bone distance	Distance from the center line between the heel and second-toe tip when the coordinate point of the talus head is projected onto the floor
GSR	Great-toe–second-toe ratio	Ratio of the distance between the second-toe tip and heel to that between the hallux tip and heel

Table 2
Participant characteristics.

		Number of subjects	Age (years)	Height (cm)	Weight (kg)	BMI
Males	Total	151	65.6 ± 11.0	166.9 ± 5.8	67.1 ± 10.2	24.0 ± 3.2
	40–64 years	50	52.5 ± 7.4	170.0 ± 5.4	72.4 ± 11.1	25.1 ± 3.9
	65–74 years	70	69.1 ± 2.9	166.7 ± 5.5	65.2 ± 9.2	23.4 ± 2.8
	>75 years	31	78.6 ± 3.7	162.5 ± 3.9	62.8 ± 7.2	23.8 ± 2.6
Females	Total	268	62.8 ± 12.4	154.4 ± 6.0	55.0 ± 9.4	23.1 ± 3.7
	40–64 years	120	51.2 ± 8.1	157.2 ± 5.3	57.6 ± 10.2	23.3 ± 4.1
	65–74 years	103	69.4 ± 2.6	153.3 ± 4.4	54.1 ± 8.2	23.1 ± 3.5
	>75 years	45	78.7 ± 3.1	149.3 ± 6.9	50.1 ± 7.3	22.5 ± 3.1

Note: All data are presented as mean ± SD.

3. Results

3.1. Feature measurement

The foot features assessed in this study included the hallux and second-toe tips, interior of the first metatarsal head, calcaneus protrusion, exterior of the fifth metatarsal head, and talus head, all of which could be detected using the proposed system. In addition, these features were identified via palpation performed by a physical therapist who understood the skeletal structure of human feet. The two sets of results demonstrated good agreement with each other, confirming the accuracy of the proposed method for foot-feature identification.

Table 3 lists the measurement results obtained using the proposed 3D foot scanner for both male and female participants. As can be observed, the results obtained for men across all age groups remain virtually consistent for all features except the GSR. However, among females, variations are observed in the NH, IS angle, MPH angle, TAL, TAH, and GFH angle across all age groups.

Table 3
Results of 3D foot-scan measurements performed using the proposed method.

	Total	40–64 years old	65–74 years old	>75 years old	F value, p value
IH	29.2 ± 2.5	29.4 ± 2.6	28.8 ± 2.3	29.5 ± 2.9	$p = 0.39$
NH	19.5 ± 2.4	19.5 ± 2.4	19.5 ± 2.3	19.6 ± 2.6	$p = 0.98$
IS angle [degrees]	133.4 ± 5.9	133.2 ± 5.6	133.5 ± 6.1	133.5 ± 6.1	$p = 0.97$
MPH angle [degrees]	33.0 ± 1.7	32.6 ± 1.8	33.1 ± 1.8	33.1 ± 1.4	$p = 0.12$
TAL	41.2 ± 2.0	40.8 ± 2.0	41.4 ± 2.1	41.5 ± 1.7	$p = 0.22$
TAH	16.2 ± 1.3	16.1 ± 1.4	16.1 ± 1.1	16.5 ± 1.5	$p = 0.26$
GFH angle [degrees]	33.0 ± 6.1	32.6 ± 5.6	33.5 ± 6.0	32.6 ± 7.2	$p = 0.65$
SHN angle [degrees]	22.2 ± 3.0	22.5 ± 3.2	22.0 ± 2.9	22.3 ± 3.1	$p = 0.64$
ABD	4.18 ± 2.53	4.37 ± 2.57	3.99 ± 2.45	4.31 ± 2.67	$p = 0.69$
GSR	0.99 ± 0.02	1.00 ± 0.02	0.99 ± 0.02	0.99 ± 0.02	$F(2148) = 4.21, p = 0.02$
BMI	24.0 ± 3.2	25.1 ± 3.9	23.4 ± 2.8	23.8 ± 2.6	$F(2147) = 4.11, p = 0.02$
Note: The above results correspond to male participants					
	Total	40–64 years old	65–74 years old	>75 years old	F value, p value
IH	28.3 ± 2.5	28.4 ± 2.5	28.3 ± 2.5	27.6 ± 2.6	$p = 0.17$
NH	18.0 ± 2.6	18.2 ± 2.4	18.3 ± 2.5	16.9 ± 3.0	$F(2265) = 4.76, p = 0.009$
IS angle [degrees]	136.1 ± 5.8	135.3 ± 5.4	135.8 ± 6.1	139.0 ± 5.6	$F(2265) = 7.08, p < 0.001$
MPH angle [degrees]	33.6 ± 2.1	33.2 ± 2.0	33.9 ± 2.3	34.2 ± 1.6	$F(2265) = 5.82, p < 0.001$
TAL	42.0 ± 2.5	41.4 ± 2.3	42.3 ± 2.7	42.7 ± 2.0	$F(2265) = 5.81, p = 0.003$
TAH	15.9 ± 1.4	16.0 ± 1.5	16.0 ± 1.3	15.3 ± 1.3	$F(2265) = 4.48, p = 0.01$
GFH angle [degrees]	35.9 ± 6.6	34.5 ± 5.5	36.1 ± 6.8	39.3 ± 7.4	$F(2265) = 9.25, p < 0.001$
SHN angle [degrees]	23.3 ± 3.4	23.1 ± 3.4	23.3 ± 3.4	23.6 ± 3.3	$p = 0.98$
ABD	4.47 ± 3.05	4.46 ± 2.79	4.43 ± 3.25	4.61 ± 3.31	$p = 0.95$
GSR	0.99 ± 0.02	0.99 ± 0.02	0.99 ± 0.02	0.99 ± 0.02	$p = 0.80$
BMI	23.1 ± 3.7	23.3 ± 4.1	23.1 ± 3.5	23.1 ± 3.7	$p = 0.40$

Note: The above results correspond to female participants. All data are presented as mean ± SD.

3.2. Correlations among features

Table 4 describes the correlation coefficients corresponding to the different foot features identified in this study. As can be observed, the GFH angle is correlated with the SHN angle, ABD, IS angle, MPH angle, TAL, TAH, and NH for both male and female participants. In addition, it is correlated with the IH among males. Meanwhile, for both participant groups, the ABD is correlated with the SHN angle, IH, and NH, whereas the NH is correlated with the TAH and IS angle. Moreover, the IS angle is correlated with the TAH, and the MPH angle is correlated with the TAL and TAH. Finally, both the TAL and BMI are correlated with the TAH.

3.3. Multiple regression analysis for GFH angle

Table 5 lists the regression results obtained for five independent foot

Table 4
Correlations between foot features, determined using Pearson's coefficient (*$p < 0.05$, **$p < 0.01$).

		1	2	3	4	5	6	7	8	9	10	11
1	GFH angle	1										
2	ABD	0.34**	1									
3	SHN angle	0.56**	0.49**	1								
4	IH	−0.23**	−0.33**	−0.13	1							
5	NH	−0.30**	−0.39**	−0.30**	0.65**	1						
6	IS angle	0.20*	0.10	0.20*	−0.74**	−0.48**	1					
7	MPH angle	0.37**	−0.07	0.13	0.11	0.01	0.01	1				
8	TAL	0.46**	−0.05	0.16*	0.10	−0.02	0.03	0.94**	1			
9	TAH	−0.15	−0.13	−0.07	0.52**	0.42**	−0.37**	0.34**	0.27**	1		
10	GSR	0.01	0.047	−0.04	0.04	−0.1	0.07	−0.12	−0.1	−0.13	1	
11	BMI	0.11	−0.01	0.02	0.01	0.06	0.07	0.07	0.12	0.34**	−0.18*	1
Note: The above results correspond to male participants												
		1	2	3	4	5	6	7	8	9	10	11
1	GFH angle	1										
2	ABD	0.26**	1									
3	SHN angle	0.51**	0.40**	1								
4	IH	−0.04	−0.34**	−0.02	1							
5	NH	−0.17**	−0.34**	−0.22**	0.49**	1						
6	IS angle	0.15*	0.04	0.10	−0.66**	−0.34**	1					
7	MPH angle	0.38**	−0.06	0.19**	0.19**	0.04	0.12*	1				
8	TAL	0.51**	−0.05	0.21**	0.20**	0.02	0.11	0.95**	1			
9	TAH	−0.15*	−0.12	−0.04	0.38**	0.40**	−0.25**	0.30**	0.22**	1		
10	GSR	0.19**	−0.04	−0.08	−0.05	−0.127	0.22**	0.03	0.11	−0.02	1	
11	BMI	−0.01	−0.02	0.03	0.07	0.07	−0.02	0.16**	0.18**	0.46**	0.01	1

Note: The above results correspond to female participants.

Table 5
Results of multiple regression analysis for GFH angle.

Variable	B	SE B	β	p value	r^2	Adjusted r^2
SHN angle	0.77	0.14	0.38	<0.001	0.54	0.52
TAL	143.02	18.56	0.47	<0.001	F for change in r2	p value
TAH	−135.65	30.51	−0.28	<0.001	33.23	<0.001
BMI	0.26	0.11	0.14	0.02		
ABD	33.58	15.96	0.14	0.04		
Note: The above results correspond to male participants						
Variable	B	SE B	β	p value	r2	Adjusted r2
SHN angle	0.72	0.10	0.37	<0.001	0.52	0.51
TAL	1.24	0.12	0.47	<0.001	F for change in r2	p value
TAH	−1.01	0.21	−0.22	<0.001	55.47	<0.001
ABD	0.26	0.10	0.12	0.01		
GSR	65.33	17.63	0.16	<0.001		

Note: The above results correspond to female participants.

features related to the GFH angle for both gender groups. Four of these features—the SHN angle, TAL, TAH, and ABD—are common for both gender groups. The BMI and GSR are also features of interest for the male and female groups, respectively. Regarding the relationship strength, the adjusted r^2 value is 0.52 and 0.51 for the male and female groups, respectively. For both groups, the GFH angle is characterized by features related to the forefoot and midfoot skeletal misalignment.

4. Discussion

In this study, a system consisting of a 3D foot scanner on a smartphone was developed to clarify the relationships between foot features and HV risk. Age-dependent foot-feature variations were observed slightly for males and distinctively for females. For females, the great toe–first metatarsal head–heel (GFH) angle associated with HV increased with age. In other words, in females, the GFH angle increased with age, suggesting that HV increased with age. Multiple regression analysis revealed that the features determining the GFH angle are the second toe–heel–navicular angle, bone distance axis, and transverse arch length and height.

Previous studies performed to assess the 3D structure of the human foot have yielded methods involving the use of depth cameras [17], deep learning [18], and Kinect [19]. The spatial accuracies afforded by such methods lie in the 1.1–3 mm range. In comparison, the proposed system offers a spatial accuracy of 1.7 mm [15]. Telfer and Woodburn investigated the effects of age, gender, shoe size, physical activity frequency, BMI, foot asymmetry, and foot loading on the foot shapes of 62 participants to identify the different foot types [12]. Varga et al. addressed whether shape descriptors derived using 3D-scan data could be used to identify differences between foot morphologies among 15 children of different ages [20]. Their results demonstrated that, with age, the feet of children grow thinner. The exact changes observed included the emergence of a bony architecture and increases in the area and concavity of the medial longitudinal arch. However, their results were obtained for a very small participant group, and no further studies were undertaken to include large-scale, HV-focused, 3D foot-surface measurements.

The measurement results obtained in this study reveal small but significant age-based variations in the identified foot features of males and females, respectively. In particular, the lower NH and increasing foot flatness among females could be attributed to aging, which does not significantly influence the SHN angle or ABD. Moreover, the longitudinal arch of the foot is likely to be connected to the tibialis posterior muscle, and the changes observed therein could be attributed to the strength of the sole muscle and transformations in the skeletal structure [21,22]. For these reasons, the lowering of the longitudinal arch is considered to be caused by the combined effect of severe tibialis-posterior-muscle impairment [23], calcaneus protrusion [24],

navicular-bone pronation [25], and aging. Moreover, the IS angle increases with aging-induced reduction in foot thickness.

The correlation coefficient between the MPH angle and TAL exceeds 0.94 (Table 4) for both gender groups, indicating a strong correlation. Among females, the TAL and TAH increase and decrease, respectively, with aging (Table 3). Because the MPH angle and TAL are skeletal features related to the forefoot width, whereas TAH is related to the forefoot height, forefoot flattening could be considered to be associated with a broad foot. Among females, the aging-induced increase in the GFH angle could be considered an early HV indicator.

Further, the foot features correlated with the GFH angle include the SHN angle and ABD, both of which are related to the midfoot. An increase in the SHN angle, which implies significant protrusion of the navicular bone, causes a corresponding increase in ABD along with an increased internal deviation of the midfoot interior. This characteristic implies that foot pronation is associated with an increase in the GFH angle, which, in turn, could cause HV. This finding is consistent with that reported by Hagedorn et al. [26], who stated that the probability of HV occurrence is high in people susceptible to foot pronation.

In addition, the ABD is correlated with the SHN angle ($r^2 > 0.40$), IH (i.e., foot-skeleton health) ($r^2 > 0.33$), and NH (i.e., longitudinal arch height) ($r^2 > 0.34$) (Table 4). These relationships suggest that the misalignment of the midfoot skeletal structure is related to foot health, which is especially true with regard to the formation of the navicular and cuneiform bones. This misalignment is influenced by both early childhood development and aging [27].

Furthermore, a correlation between IH and TAH is observed in both the male ($r^2 = 0.52$) and female ($r^2 = 0.38$) participant groups (Table 4). A low correlation is observed among females because the transverse arch reflected by the TAH is strongly influenced by female footwear.

Finally, with regard to flat feet, i.e., fallen longitudinal arches, several extant articles have reported on footprints [28]. From a biomechanics perspective, the impairment of the tibialis posterior muscle or muscles in the sole could be considered the main cause of flat feet [29]. Under pronation—the decrease in the position of the navicular bone to which the tibialis posterior muscle attaches—several 3D changes occur, such as subtalar-joint and forefoot supination and navicular-bone pronation. Therefore, the facilitation of comprehensive 3D foot-feature assessment for effective pronation diagnosis is a major benefit offered by the proposed system.

Table 5 indicates that the SHN angle and ABD are dominant midfoot-related skeletal features for determining the GFH angle for both gender groups. Further, the TAL and TAH are corresponding dominant forefoot-related features. The BMI and GSR are other dominant features in the male and female participant groups, respectively. The results of the multiple regression analysis performed in this study reveal adjusted determination coefficient values of 0.52 and 0.51 for the male and female participant groups, respectively. During this analysis, no multicollinearity was confirmed with respect to any independent feature. Moreover, large values of β corresponding to the SHN angle and TAL were observed for the male and female participant groups, respectively.

Regarding the features associated with HV, prior studies have revealed a low BMI and high heel usage among females aged 20–64 years, whereas a high BMI and flat feet were observed among males [2, 13]. These results suggest that the etiologic mechanisms of HV occurrence in males and females differ significantly. Although no overweight or underweight participants were recruited in this study, the results obtained reveal a correlation between BMI with HV among males, albeit not as strong as that reported previously by Nguyen et al. [2].

Further, King and Toolan reported that, compared to the control group (individuals without HV), males and females diagnosed with HV are characterized by increased protrusion of the first metatarsal and elongated first metatarsal and proximal phalanx of the hallux [4]. Therefore, the first toe plays a key role in HV diagnosis. In contrast, the findings of this study reveal that a long second toe is associated with a large GFH angle; in other words, the second toe plays a key role in HV diagnosis. King and Toolan compared the lengths of the first and second metatarsals, whereas in this study, we compared the distances between the first- and second-toe tips and heel. As HV develops, the proximal phalanx of the hallux deviates laterally toward the second toe, reducing the distance between the hallux tip and heel and causing the second toe to appear longer.

The findings of this study reveal that the GFH angle (as an HV index) is influenced by forefoot flatness and misalignment of the midfoot skeleton. Komeda et al. considered the NH to be an index of flat feet, which influences HV [30]. However, in this study, the SHN angle was identified as an independent variable via multiple regression analysis. Because the SHN angle and NH are inversely correlated, it is obvious that both the height and position of the navicular bone can be considered key HV features. It is noteworthy that, being 3D, the SHN angle cannot be determined using 2D measurement systems. However, the proposed 3D-scanning system can easily evaluate both the NH and SHN angle via the use of an automatically constructed 3D foot model.

Thus, using the proposed smartphone-based 3D foot scanner, we successfully implemented a quantitative method for assessing the human foot structure, which helped us identify factors influencing HV occurrence.

This study is limited by several factors. First, all measurements were performed on the exterior surfaces of the feet of the participants. Therefore, there may exist differences between the GFH and HV angles measured via X-ray and the proposed approach. In addition, all measurements in this study were performed manually; therefore, the measured data are susceptible to hand vibrations and disturbances during video recording. Lastly, the 3D foot model considered in this study was constructed using 2D images; hence, the construction process is prone to errors.

Conclusions

This paper presented a smartphone-based 3D foot-scanning method to analyze the structure of the human foot. The SHN angle and ABD were identified as dominant midfoot skeletal features for determining the HV-related GFH angle. Correspondingly, the TAH and TAL were identified as the dominant forefoot-related features. Moreover, this study revealed the occurrence of negligible and significant age-based variations in the identified foot features among males and females, respectively. The findings of this study reveal that it is possible to perform non-invasive assessments of the human foot structure using a simple smartphone application. This work will facilitate the identification of parameters concerning the skeletal structure of the human foot and their contributions to HV occurrence. Thus, the results obtained in this study can be considered to constitute a significant step toward HV prevention.

Author contributions

TY and KY planned the study, supervised the data analysis, and wrote the paper. TY, KY, MS, and MK performed all measurements and contributed to the data acquisition. TY, KY, MS, MK, and SA performed all statistical analyses and contributed to revising the paper. MK and SA helped plan the study, including the instrumentation and revision of the manuscript.

Declaration of Competing Interests

There are no conflicts of interest to declare.

Acknowledgments

Not applicable.

Funding

This work was supported by JSPS KAKENHI [Grant Nos. 18H03559, 18K12161], CASIO Science Promotion Foundation. The funding sources had no involvement in the study design; data collection, analysis, or interpretation; writing of the report; or decision to submit the article for publication.

Ethics

The study was approved by the University Hospital Medical Information Network Registry of Ryotokuji University (Approval Number 1909; Trial registration number UMIN000037694), and written informed consent was obtained from the participants.

Supplementary materials

Supplementary material associated with this article can be found, in the online version, at doi:10.1016/j.medengphy.2021.08.001.

References

[1] Nix S, Smith M, Vicenzino B. Prevalence of hallux valgus in the general population: a systematic review and meta-analysis. J Foot Ankle Res 2010;3:21.
[2] Nguyen US, Hillstrom HJ, Li W, Dufour AB, Kiel DP, Procter-Gray E, et al. Factors associated with hallux valgus in a population-based study of older women and men: the MOBILIZE Boston Study. Osteoarthritis Cartilage 2010;18:41–6.
[3] Menz HB, Roddy E, Thomas E, Croft PR. Impact of hallux valgus severity on general and foot-specific health-related quality of life. Arthritis Care Res (Hoboken) 2011; 63:396–404.
[4] King DM, Toolan BC. Associated deformities and hypermobility in hallux valgus: an investigation with weightbearing radiographs. Foot Ankle Int 2004;25:251–5.
[5] Roddy E1, Zhang W, Doherty M. Prevalence and associations of hallux valgus in a primary care population. Arthritis Rheum 2008;59:857–62.
[6] Nishimura A, Fukuda A, Nakazora S, Uchida A, Sudo A, Kato K, et al. Prevalence of hallux valgus and risk factors among Japanese community dwellers. J Orthop Sci 2014;19(2):257–62.
[7] Menz HB, Morris ME. Footwear characteristics and foot problems in older people. Gerontology 2005;51:346–51.
[8] Galica AM, Hagedorn TJ, Dufour AB, Riskowski JL, Hillstrom HJ, Casey VA, et al. Hallux valgus and plantar pressure loading: the FraminGFH anglem foot study. J Foot Ankle Res 2013;6:42.
[9] Telfer S, Woodburn J. The use of 3D surface scanning for the measurement and assessment of the human foot. J Foot Ankle Res 2010;3:19.
[10] Stanković K, Booth GB, Danckaers F, Burg F, Vermaelen P, Duerinck S, et al. Three-dimensional quantitative analysis of healthy foot shape: a proof of concept study. J Foot Ankle Res 2018;11:8.
[11] Nix SE, Vicenzino BT, Collins NJ, Smith MD. Characteristics of foot structure and footwear associated with hallux valgus: a systematic review. Osteoarthritis Cartilage 2012;20:1059–74.
[12] Telfer S, Woodburn J. The use of 3D surface scanning for the measurement and assessment of the human foot. J Foot Ankle Res 2010;3:19–27.
[13] Mall NA, Hardaker WM, Nunley JA, Queen RM. The reliability and reproducibility of foot type measurements using a mirrored foot photo box and digital photography compared to caliper measurements. J Biomech 2007;40(5):1171–6.
[14] Zhao J, Xiong S, Bu Y, Goonetilleke RS. Computerized girth determination for custom footwear manufacture. Comput Ind Eng 2008;54(3):359–73.
[15] Yamashita K, Yamashita T, Sato M, Kawasumi M, Takase Y. Development of a quantitative measurement system for three-dimensional analysis of foot morphology using a smartphone. Conf Proc IEEE Eng Med Biol Soc 2019.
[16] Pique-Vidal C, Vila J. A geometric analysis of hallux valgus: correlation with clinical assessment of severity. J Foot Ankle Res 2009;2:15.
[17] Kobayashi T, Ienaga N, Sugiura Y, Saito H, Miyata N, Tada M. A simple 3D scanning system of the human foot using a smartphone with depth camera. In: Proceedings of 3DBody Tech; 2018.
[18] Lunscher N, John Z. Deep learning anthropomorphic 3D point clouds from a single depth map camera viewpoint. In: Proceeding of the IEEE International Conference on Computer Vision Workshops; 2017. p. 689–96.
[19] Rogati G, Leardini A, Ortolani M, Caravaggi P. Validation of a novel Kinect-based device for 3D scanning of the foot plantar surface in weight-bearing. J Foot Ankle Res 2019;12:46.
[20] Varga M, Price C, Morrison CS. Three-dimensional foot shape analysis in children: a pilot analysis using three-dimensional shape descriptors. J Foot Ankle Res 2020; 13:6.
[21] Vicenzino B, Griffiths SR, Griffiths LA, Hadley A. Effect of antipronation tape and temporary orthotic on vertical navicular height before and after exercise. J Orthop Sports Phys Ther 2000;30:333–9.
[22] Mueller TA, Host JV, Norton BJ. Navicular drop as a composite measure of excessive pronation. J Am Podiatr Med Assoc 1993;83:198–202.
[23] Arangio GA, Salathe EP. A biomechanical analysis of posterior tibial tendon dysfunction, medial displacement calcaneal osteotomy and flexor digitorum longus transfer in adult acquired flat foot. Clin Biomech 2009;24(4):385–90.
[24] Caravaggi P, Sforza C, Leardini A, Portinaro N, Panou A. Effect of plano-valgus foot posture on midfoot kinematics during barefoot walking in an adolescent population. J Foot Ankle Res 2018;11:55.
[25] Lange B, Chipchase L, Evans A. The effect of low-dye taping on plantar pressures, during gait, in subjects with navicular drop exceeding 10mm. J Orthop Sports Phys Ther 2004;34:201–9.
[26] Hagedorn TJ, Dufour AB, Riskowski JL, Hillstrom HJ, Menz HB, Casey VA, et al. Foot disorders, foot posture, and foot function: the Framingham foot study. PLoS ONE 2013;8(9):e74364.
[27] Heuck FHW, Bast BRG. Radiologische skizzen und tabellen. peripheres skelett. Stuttgart New York: Thieme; 1994.
[28] Woźniacka R, Bac A, Matusik S, Szczygieł E, Ciszek E. Body weight and the medial longitudinal foot arch: high-arched foot, a hidden problem? Eur J Pediatr 2013;172 (5):683–91.
[29] Watanabe K, Kitaoka HB, Fujii T, Crevoisier X, Berglund LJ, Zhao KD, et al. Posterior tibial tendon dysfunction and flatfoot: analysis with simulated walking. Gait Posture 2013;37:264–8.
[30] Komeda T, Tanaka Y, Takakura Y, Fujii T, Samoto N, Tamai S. Evaluation of the longitudinal arch of the foot with hallux valgus using a newly developed two-dimensional coordinate system. J Orthop Sci 2001;6:110–8.